https://doi.org/10.25686/10.25686.2022.67.40.002

# ECOLOGICAL SECURITY ASSESSMENT MODEL FOR THE CITY OF MATLOSANA MUNICIPALITY IN THE NORTH WEST PROVINCE, SOUTH AFRICA

J. Cole, S. Sogayise, N. Dudumashe, M. Sethobya Council for Geoscience, Pretoria, South Africa

An ecological security assessment model was created for the City of Matlosana Municipality in the North West Province of South Africa for 2001, 2014, 2016, 2018 and 2020. The pressure-state-response model considered the climate, mining activities, and population density to be the drivers that place pressure on the ecological security of the municipality. Indicators of the pressures on and state and response of the environment were derived from remote sensing data sets, including Landsat, Sentinel-2 and MODIS satellites, and world population density and rainfall data provided by various organisations. Principal component analysis was used to determine the indicator weights. Roughly 30 % of the municipality, has low to very low ecological security. These areas cover the north and south of the municipality with the central region generally more ecologically secure. Towns and mining areas are the most vulnerable, but they constitute only up to 5 % of the municipal area. Two potential ecologically vulnerable areas were identified, one in the northwest and another in the extreme southern section of the municipality.

**Keywords:** ecological security, remote sensing, satellite images, PSR model, PCA.

## Introduction

A very effective way to assess and monitor the impact of Land Use and Land Cover (LULC) change on the environment is through ecological security assessment models. The models evaluate ecological indicators that provide information about the attributes and conditions of an ecosystem (Longstaff et al., 2010). They relate the impact of selected pressures to current conditions and the actions taken to maintain or restore the ecosystem's health. An ecosystem is a community or selection of communities (e.g. human, animal, plant life, micro-organisms, etc.) that interacts with the environment (Freedman, 1998). Numerous models exist, but one of the most commonly used is the Pressure-State-Response (PSR) model developed by the Organisation for Economic Cooperation and Development (OECD) (Linster, Fletcher, 2001). This models the interaction between external pressures on an ecosystem, the current state of the system, and the way in which the ecosystem responds to the pressures.

The first step is to identify factors that put pressure on the ecosystem, establish indicators that can be used to measure these, and select appropriate data sets from which they can be extracted. The second set of indicators reports on the current state of the ecosystem. It assesses specific aspects of the ecosystem that will be affected by the previously identified pressures. The last step is to select indicators that give information about the response of the ecosystem. These are measurable quantities that quantify improvements or deteriorations in the ecosystem and can be used to flag areas of concern.

# Study area

The City of Matlosana Municipality is located in the southeast of the North West Province, South Africa (Fig. 1a). It covers the area of 3 617 km2. Summers are generally warm to hot (November to February) and winters are cool and dry (May to August). The relief decreases from northwest to southeast (Fig. 1b). Numerous rivers flow through the municipality and the Vaal River, from which the municipality gets its water (Annual Report 2020-2021), forms the south-eastern boundary of the municipality (Fig. 1c). Grasslands and thornvelds cover most of the area (Fig. 1d).

Farming is widespread in the municipality, ranging from cattle and game farming in the drier west, maize and wheat in the central and southern regions, and a variety of crops in the wetter east and northeast. Gold mining is prevalent in the Klerksdorp-Orkney-Stilfontein area in the east of the municipality. Hartbeesfontein, where mining also takes place, is located about 28 km northwest of Klerksdorp.

The municipality has a population of 447,000 people, with 89.4% urban and 10.6 % rural residents (Annual Report, 2021). This equates to a population density of 124 people per km<sup>2</sup>.

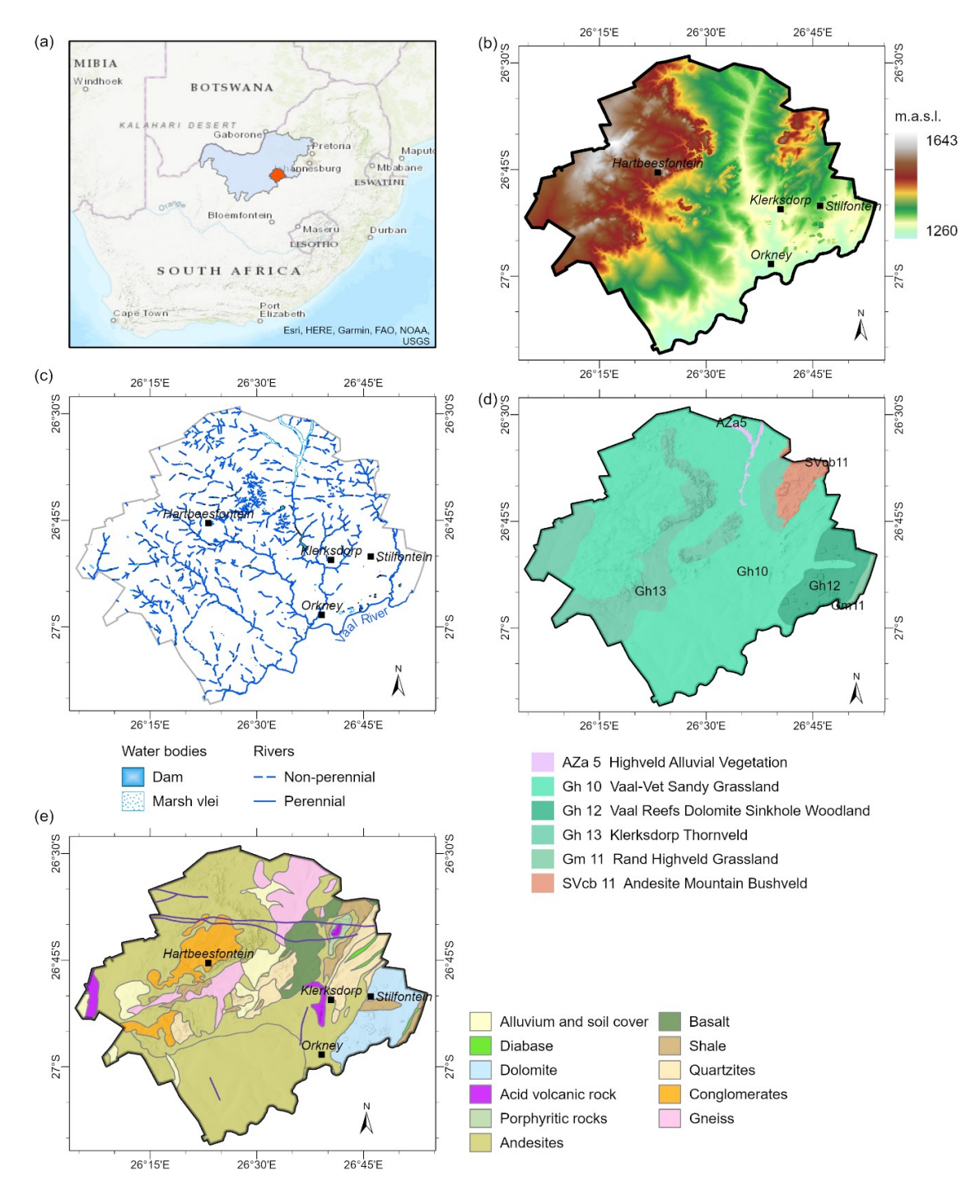


Fig. 1. (a) Locality map of the City of Matlosana Municipality. The blue polygon shows the North West Province, and the orange polygon is the Matlosana Municipality; (b) Digital elevation model; (c) Drainage system; (d) Biomes (SANBI 2006-2018); (e) Dominant lithologies in the Matlosana Municipality (CGS, 2019)

# Material and methods

A PSR model was developed for the Matlosana Municipality (Fig. 2). Pressure indicators include climatic conditions, mining activities, and population growth. A regional vegetation health study of the North West Province showed that the impact of climatic changes constituted a definite risk to agricultural activities and the environment in general (Cole, Sogayise, Dudumashe, 2021). Mining activities provide additional pressures in the form of subsidence due to a drop in the groundwater table resulting from pumping in the mines, pollution in the form of acid mine drainage, and changes in vegetation due to physical mining activities. Increasing population density is the third major pressure.

Climactic conditions, mining activity, and population density pressures impact vegetation health, soil moisture conditions, LULC, and the general population. Changes in these parameters give an indication of the condition of the ecosystem.

The response of the ecosystem to the pressures considers human actions to deal with negative pressure and the natural response of vegetation to these mitigating actions. The responses to the identified pressures are:

- stable agricultural activity despite droughts;
- rehabilitation at mines, and
- increased living standards for the general population.

Socio-economic conditions in the municipality affect the consideration of whether certain impacts are positive or negative. In most ecological sensitivity studies, any impact on the natural environment is generally considered negative. However, due to the level of poverty in large parts of the municipality, increased housing must be considered a positive response since it indicates improved living conditions. Similarly, farming in the North West Province is important to the national economy and food security in general. Although farming may adversely affect biodiversity, it is an important contributor to the economic well-being of the region.

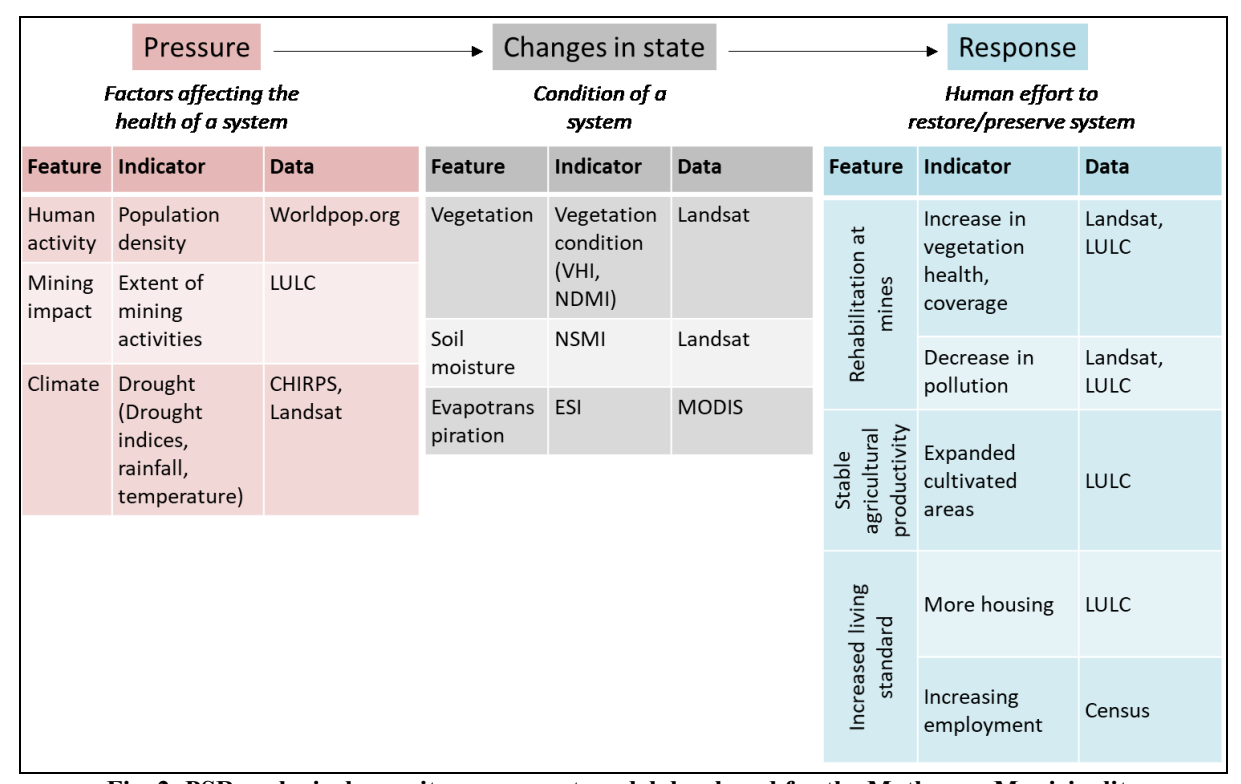


Fig. 2. PSR ecological security assessment model developed for the Matlosana Municipality

# Data

An important requirement for the model is that historical data must be available to establish change patterns, and the data must also be regularly updated to allow for continuous monitoring. In this context, satellite remote sensing is ideal as it continuously collects vast quantities of data, and many satellites have been active for multiple years and even decades. The major drawback with satellite remote sensing data is cloud cover. For a change detection study, data from the same period of each year must be compared to remove the effects of seasonal changes.

For this study, the joint NASA and USGS Landsat programme is the primary data source. The satellite has bands in the visible, near infrared, short wave infrared and thermal infrared wavelength ranges. The spatial resolution of 30 m for the optical data also allows for detailed studies. Landsat thermal data have a resolution of 100 m.

Landsat does not provide data for all indicators, and additional data sources were used. Unfortunately, these data sets generally have very low spatial resolution. Rainfall data with a spatial resolution of about 5 km were obtained from the Climate Hazards group Infrared Precipitation with Stations CHIRPS) (Funk et al., 2015). The MODIS (Moderate Resolution Imaging Spectroradiometer) sensor aboard the Terra satellite provided evapotranspiration data with a spatial resolution of 500 m (Running, Mu, Zhao, 2017).

Even though Landsat data cover such a long time period, MODIS and world population density data (WorldPop, 2018) are only available from 2000, thus restricting the temporal extent of the study.

For the Matlosana Municipality, ample cloud-free Landsat scenes are available for the dry season (June-September), but to study vegetation health it is necessary to look at times of the year where vegetation is expected to be healthy, i.e., the wet season (October–March). Naturally, the rainy season will have regular cloud cover. It was impossible to find satellite scenes at the peak of the rainy season that were cloud free over multiple years, and as a result, data from just after the wet season had to be used. This is during the month of May in the study area. Cloud-free optical satellite imagery was available for 2001, 2014, 2016, 2018, and 2020 (Table 1). Every effort was made to obtain scenes collected roughly at the same time each year, but for 2016, the only cloud free scene was recorded on 4 May. This may result in vegetation indices appearing healthier due to the earlier date and not general drought conditions during the other years. Two scenes (171-078 and 171-079) cover the Matlosana Municipality.

Landsat scenes used in this study

Table 1

Scene	Date	
LE07_L2SP_171078_20010604_20200917_02_T1	4 Jun 2001	
LE07_L2SP_171079_20010604_20200917_02_T1		
LC08_L2SP_171078_20140531_20200911_02_T1	31 May 2014	
LC08_L2SP_171079_20140531_20200911_02_T1		
LC08_L2SP_171078_20160520_20200906_02_T1	20 May 2016	
LC08_L2SP_171079_20160520_20200906_02_T1		
LC08_L2SP_171078_20180526_20200901_02_T1	26 May 2018	
LC08_L2SP_171079_20180526_20200901_02_T1		
LC08_L2SP_171078_20200531_20200820_02_T1	31 May 2020	
LC08_L2SP_171079_20200531_20200820_02_T1		

MODIS evapotranspiration data (MOD16A2v6) were selected to cover the same periods (tTable 2). Each data set comprises data averaged over an eight-day period.

# MODIS scenes used in this study

Scene	Date
MOD16A2.A2001153.h20v11.006	25 May - 1 June 2014
MOD16A2.A2014145.h20v11.006	25 May - 1 June 2014
MOD16A2.A2016137.h20v11.006.	16 – 23 May 2016
MOD16A2.A2018145.h20v11.006	25 May - 1 June 2018
MOD16A2.A2020145.h20v11.006	24 – 31 May 2020

The LULC classifications form a critical part of the ecological security assessment. The increase or decrease in certain cover types can have a significant influence on the assessment. For example, increasing mining may lead to more pollution, land degradation and hazards such as subsidence. However, due to the socioeconomic situation in the municipality, the impact of land cover types is not simply that more natural vegetation implies better ecological security. Improved living conditions will have a positive effect on the environment, but this means more houses and less natural vegetation.

The LULC data sets are qualitative, and to use them in the ecological security assessment model, scores or values were assigned to the LULC types in a way that is applicable to a specific indicator. For example, mining areas will have a significant negative impact on the environment and will be assigned a high value where it is a pressure indicator, while wetlands, grasslands, etc., will be assigned a low value.

The data and derived products used in the PSR model are listed in Table 3.

Table 3

Data and derived products used in the PSR model (Fig. 2)

Indicator category	Indicator	Data (resolution)	Effect <sup>a</sup>
Human activity	Population density	WorldPop.org (90 m)	-
Mining impact	Extent of mining activity	LULC (10 m and 30 m)	-
Climate	Modified visible and shortwave infrared drought	Landsat (30 m)	+
	Rainfall	CHIRPS (~5000 m)	+
	Temperature	Landsat (30 m)	-
Vegetation	Vegetation health index (Bento et al., 2018). See	Landsat (30 m)	+
		Landsat (30 m)	+
Soil moisture		Landsat (30 m)	+
Evapotranspiration		MODIS	-
		Landsat (30 m)	+
mines			
		Landsat (30 m)	-
Stable agricultural productivity	Expanded cultivated areas	LULC (10 m and 30 m)	+
Increased living standards	More housing	LULC (10 m and 30 m)	+
	Increasing employment (Statistics South Africa,	Census and other	+
		government data	
	Quarter 2 of 2017-2018, 2017; EDR, Quarter 2 of		
	2018-2019, 2018; EDR, Quarter 2 of 2021-2022,		
	Human activity Mining impact Climate  Vegetation  Soil moisture  Evapotranspiration  Rehabilitation at mines  Stable agricultural productivity	Human activity Mining impact Climate Modified visible and shortwave infrared drought index (Sun et al., 2021). See equation (A.1).  Rainfall Temperature  Vegetation Vegetation health index (Bento et al., 2018). See equation (A.2).  Normalised difference moisture index (Zhang et al., 2016). See equation (A.5).  Soil moisture Normalised difference soil moisture index (Haubrock et al., 2008). See equation (A.6).  Evapotranspiration Evaporative stress index (Qiu et al., 2021). See equation (A.7).  Rehabilitation at mines Modified soil adjusted vegetation index in mining areas (Qi et al., 1994). See equation (A.8).  Iron pollution in mining areas. See equation (A.9).  Stable agricultural productivity Increased living standards  Increasing employment (Statistics South Africa, 2011; EDR, Quarter 2 of 2015-2016, 2015; EDR, Quarter 2 of 2017-2018, 2017; EDR, Quarter 2 of	Human activity  Mining impact  Extent of mining activity  Climate  Modified visible and shortwave infrared drought index (Sun et al., 2021). See equation (A.1).  Rainfall  Vegetation  Vegetation  Vegetation health index (Bento et al., 2018). See equation (A.2).  Normalised difference moisture index (Zhang et al., 2016). See equation (A.5).  Soil moisture  Normalised difference soil moisture index (Haubrock et al., 2008). See equation (A.6).  Evapotranspiration  Evaporative stress index (Qiu et al., 2021). See equation (A.7).  Rehabilitation at mines  Modified soil adjusted vegetation index in mining areas (Q i et al., 1994). See equation (A.8).  Iron pollution in mining areas. See equation (A.9).  Stable agricultural productivity  Increased living standards  Increasing employment (Statistics South Africa, 2011; EDR, Quarter 2 of 2017-2018, 2017; EDR, Quarter 2 of 2015-2016, 2015; EDR, Quarter 2 of 2018-2019, 2018; EDR, Quarter 2 of 2021-2022,

A positive effect: The greater the value the more positive the impact is, Negative effect: The greater the value the more negative the impact is

# **Data preparation**

# Spatial resolution

The data sets have varying resolutions (Table 3) and must be resampled to the required resolution for the model. Most of the indicators were derived from 30 m Landsat data, and since a major focus of the study is on the impact of mining on the ecological system, it is preferable to keep the resolution this high. Acid mine drainage may be restricted to localised zones and will be better detected by higher spatial resolution data.

# Normalisation

The indicators measure different types of parameters with different value ranges and need to be normalised to ensure that all indicators contribute to a parameter equally. To identify vulnerable areas, indicator values need to be normalised according to whether they have a positive or negative effect on the ecosystem (Bai, Tang, 2010) (Table 3).

For positive indicators, the normalisation equation is

$$Y_{i} = \frac{X_{i} - X_{\min}}{X_{\max} - X_{\min}} \tag{1}$$

and for negative indicators it is

$$Y_i = \frac{X_{\text{max}} - X_i}{X_{\text{max}} - X_{\text{min}}} \tag{2}$$

where Xmax and Xmin are the maximum and minimum values of the indicator over the whole study period, and Xi is the indicator value for each year (Wang, Sun, Wu, 2018).

## Indicator independence

To avoid statistical bias, it is necessary to ensure that the indicators are independent of each other. The Pearson correlation coefficient between the indicators was calculated using the utility in PyGMI, an open-source software package (http://patrick-cole.github.io/pygmi/). The formula is (Johnson, Wichern, 1998):

$$r_{xy} = \frac{\sum_{i=1}^{n} (X_i - \text{mean}(X_i))(Y_i - \text{mean}(Y_i))}{\sqrt{\sum_{i=1}^{n} (X_i - \text{mean}(X_i))^2} \sqrt{\sum_{i=1}^{n} (Y_i - \text{mean}(Y_i))^2}}$$
(3)

where Xi and Yi are the two indicators being compared, and n is the sample size.

The correlation coefficients calculated for the indicators are very low, with closest to zero. Higher correlations of 0.35 to 0.67 occurred between the drought index (MSVDI1, equation A.1) and soil moisture index (NSMI, equation A.6), and LST and MSVDI1 also saw correlations between 0.46 and 0.51. The correlation coefficients are low enough to assume that the data sets are independent.

### Weighting

Each indicator in the ecological security model must be given a weight. For this study, the weights were derived from the data using principal component analysis. Each principal component contains contributions from all the bands in the original data set, but they are uncorrelated with each other and have variances equal to the eigenvalues of the covariance matrix (Johnson, Wichern, 1998). The eigenvectors of the covariance matrix are the principal components, with the first component containing the most variance, followed by the second, third, and so on.

By dividing each eigenvalue (principal component) by the sum of all eigenvalues, it is possible to determine the percentage of variance (and therefore information) that a component contains. This is called the contribution rate, and often only the first components which cumulatively contain 85 % of the information are retained (Zou et al., 2021). Indicator weights are then calculated using the following equations (Zou et al., 2021; Ding et al., 2018):

$$H_i = \sum_{k=1}^{m} \lambda_{ik}^2 \tag{4}$$

where i is the indicator number and k is the number of retained principal components. lik is the eigenvalue of indicator i with respect to principal component k. Hi is the variance of indicator i.

$$w_i = H_i / \sum_{i=1}^n H_i \tag{5}$$

where wi is the weight for indicator i, and n is the number of indicators.

Since PCA is data-driven, a set of weights is calculated for each year. The moisture indices (NDMI, NMSI) and the percentage of economically active people consistently have zero weight (Fig. 3). With a few exceptions, the weights are relatively consistent over the different years. Exceptions are the impact of mining areas that had larger weights in 2001 to 2016 but decreased significantly in 2018 and 2020, and rainfall that varied between 0.00026 in 2016 and 0.24944 in 2018.

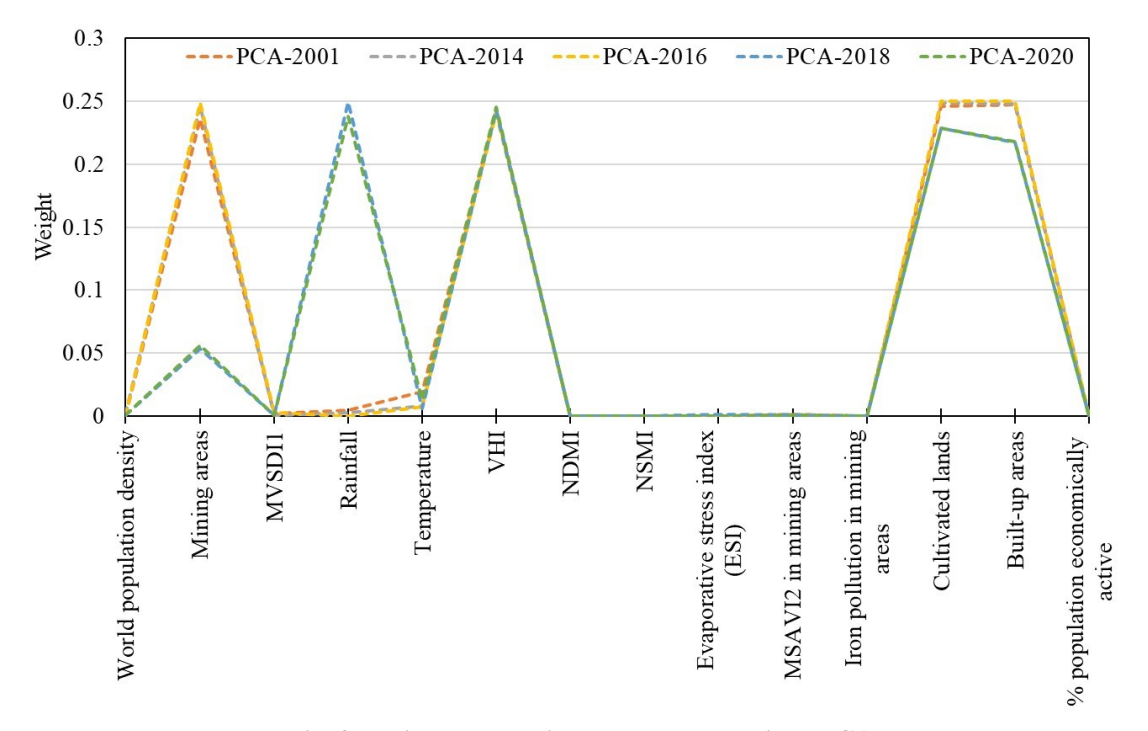


Fig. 3. Weights determined by the data-driven PCA method

### Results and discussion

The results of the ecological security assessment were classified using natural break classification to divide the data for each year into five natural groupings (Shao) et al., 2014) and these were then assigned ecological security grades of very low, low, moderate, high, and very high

(Fig. 4). The KOSH mining area consistently has the lowest ecological security. In 2001, the southern and north-eastern regions of the municipality were also quite vulnerable. The security improved in 2016 with only the mining areas showing very low security. This is an unexpected result since 2016 experienced low rainfall, similar to 2001 and 2014. The vegetation health index was higher for 2016 than for the previous years and was the source of the improved ecological security. This index was most probably higher since the Landsat scene for 2016 was collected on 4 May, whereas the scenes for the other years were collected in late May and early June.

A new area with very low ecological security appeared in the northwest in 2018. It was still present in 2020, but the extent decreased. Overall, the central belt of the municipality remained ecologically secure from 2016 to 2020.

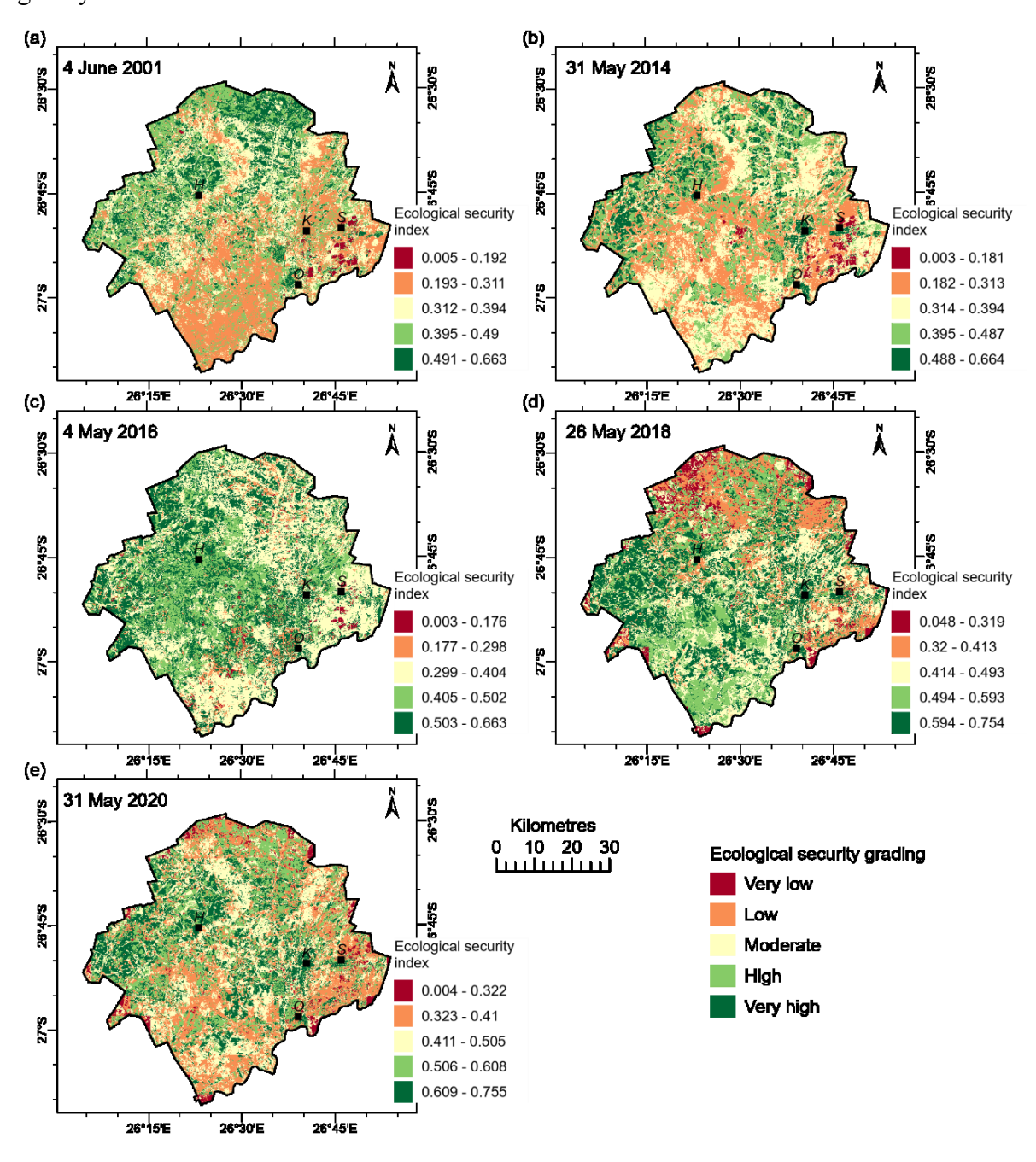


Fig. 4. Ecological security assessment models for the Matlosana Municipality using weights determined from PCA

The PCA-weighted model shows between 13 % and 30 % of the municipality to have very high ecological security and a further 20 % to 25 % with high security (Fig. 5). These areas fall predominantly in the central section of the region and correspond to cultivated areas and grasslands. In 2014, these areas covered 30 % of the area, compared to almost 40 % to 50 % in the other years. From the rainfall, land surface temperature, and modified visible and shortwave drought index, we know that this was a dry year, explaining the pressure on the ecological security index.

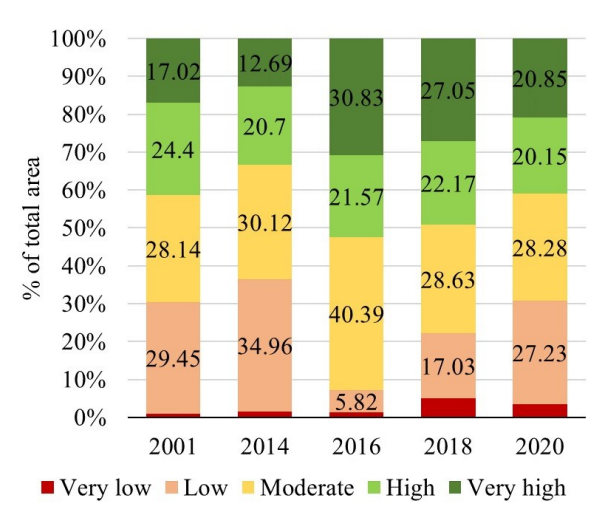


Fig. 5. Area proportions of the different ecological security grades

20-35 % of the Matlosana Municipality has low to very low ecological security. The most vulnerable areas are around the towns and mines, and it is clearly due to the mining activity and population density pressure indicators. The areas with low ecological security are much more widespread and are more related to the climactic conditions under which they occur. LULC maps classified the south as mostly grasslands, but in the north, there is a mixture of farmlands and grasslands.

Two areas of concern have become apparent from the modelling results. A highly vulnerable area in the northwest of the municipality in 2018 appears to be due to low vegetation health index values. The VHI increased in 2020 but the ecological security remained extremely low, albeit within a smaller extent. The other area of interest is the southernmost tip of the municipality. Here, the VHI is high and the reason for the vulnerability is unclear.

### **Conclusions**

The first ecological security assessment model developed for the Matlosana Municipality identified areas with low security. However, during the modelling process, the following factors affecting the modelling outcome were identified:

- Cloud-free scenes for the same time over the study period were only available for times after the rainy season when vegetation is already decreasing and crops have been harvested;
- The limited number of spectral bands available in Landsat data leads to ambiguity in some of the indices that were calculated;
  - The LULC classification yielded many misclassifications;
- The Landsat scenes used in the temporal study must be collected as close as possible to the same date of each year to avoid seasonal changes affecting the result.

Despite these factors, the process of developing and implementing an ecological security assessment model is now well understood, and once these factors have been addressed, the model

can be adapted if required and rerun. The effect of different indicators can be tested, and modelling can also be applied to other areas.

This research was undertaken under the funding instrument for the BRICS Multilateral Joint Science and Technology Research Collaboration between South Africa (supported by the National Research Foundation (NRF)), Russia (supported by the Russian Foundation for Basic Research (RFBR)) and China (supported by the National Natural Science Foundation of China (NSFC)). The NRF is hereby duly acknowledged for its financial grant (NRF grant No: 120456). The authors would like to register their sincere thanks to the Council for Geoscience (CGS) for providing an opportunity and various resources to undertake this study/research.

# **Appendix**

Modified visible and shortwave infrared drought index (Sun et al., 2021):

$$MVSDI1 = 1 - ((SWIR2 - Blue) + (SWIR1 - Blue) + (Red - Blue))$$
(A.1)

Vegetation health index (Bento et al., 2018):

$$VHI = \alpha VCI + (1 - \alpha)TCI$$
(A.2)

where  $\alpha$  is the contribution of each condition index to the VHI. This is normally unknown and a value of 0.5 is commonly used.

$$VCI = \frac{VI - VI_{\min}}{VI_{\max} - VI_{\min}} \tag{A.3}$$
 where VI is a vegetation index, and VImax and VImin are the minimum and maximum values of

where VI is a vegetation index, and VImax and VImin are the minimum and maximum values of the VI for a pixel over the observation period.

$$TCI = \frac{LST_{max} - LST}{LST_{max} - LST_{min}}$$
(A.4)

where LSTmax and LSTmin are the minimum and maximum values of land surface temperature for a pixel over the observation period.

Normalised difference moisture index (Zhang et al., 2016):

$$NDMI = \frac{NIR - SWIR1}{NIR + SWIR1}$$
 (A.5)

Normalised difference soil moisture index (Haubrock et al., 2008):

$$NSMI = \frac{SWIR1 - SWIR2}{SWIR1 + SWIR2}$$
(A.6)

Evaporative stress index (Qiu et al., 2021):

$$ESI = 1 - \left(\frac{ET}{PET}\right) \tag{A.7}$$

where ET is evapotranspiration and PET is potential evapotranspiration provided by MODIS. Modified soil adjusted vegetation index (Qi et al., 1994):

$$MSAVI2 = 0.5 \left[ 2NIR + 1 - \sqrt{(2NIR + 1)^2 - 8(NIR - RED)} \right]$$
 (A.8)

Iron oxide ratio:

$$FeO = \frac{NIR}{Green} \tag{A.9}$$

### References

- 1. Bai X., Tang J. Ecological security assessment of Tianjin by PSR model. *Procedia Environmental Sciences*, 2010. Vol. 2, P. 881–887. https://doi.org/10.1016/j.proenv.2010.10.099.
- 2. Bento V. A., Trigo I. F., Gouveia C. M., DaCamara C. C. Contribution of Land Surface Temperature (TCI) to Vegetation Health Index: A comparative study using clear sky and all-weather climate data records. *Remote Sensing*, 2018. Vol. 10, No. 9, 1324. https://doi.org/10.3390/rs10091324.

- 3. Annual Report 2020-2021. City of Matlosana, 2021, 456 pp. Available at: https://www.matlosana.gov.za/AnnualReportss.html.
- 4. Cole J., Sogayise S., Dudumashe N. An overview of vegetation health in the North West Province, South Africa, between 2010 and 2020. *IOP Conference Series: Earth and Environmental Science*, 2021. 932, 012004. https://doi.org/10.1088/1755-1315/932/1/012004.
- 5. Ding Q., Shi X., Zhuang D., Wang Y. Temporal and spatial distributions of ecological vulnerability under the influence of natural and anthropogenic factors in an eco-province under construction in China. *Sustainability*. 2018 Vol. 10, No. 9. https://doi.org/10.3390/su10093087.
- 6. Freedman B. Environmental Science: A Canadian Perspective. Dalhouse University Libraries Digital Editions, Halifax, NS, Canada, 1998, 885 pp. Available at: https://ecampusontario.pressbooks.pub/environmentalscience/
- 7. Funk C., Peterson P., Landsfeld M., Pedreros D., Verdin J., Shukla S. et el. The climate hazards infrared precipitation with stations a new environmental record for monitoring extremes. *Scientific Data*, 2015. Vol. 2, 150066. https://doi.org/10.1038/sdata.2015.66.
- 8. Haubrock S. N., Chabrillat S., Lemmnitz C., Kaufmann H. Surface soil moisture quantification models from reflectance data under field conditions. *International Journal of Remote Sensing*, 2008. Vol. 29, No. 1. P. 3–29 https://doi.org/10.1080/01431160701294695.
- 9. Johnson R. A., Wichern D. W. Applied Multivariate Statistical Analysis. Prentice Hall, New Jersey, 1998. 816 pp. http://dx.doi.org/10.2307/2533879.
- 10. Linster M., Fletcher J. Using the Pressure-State-Response Model To Develop Indicators of Sustainability. Organization for Economic Co-operation and Development, Paris, 2001 P.1–11. Available at: http://www.oecd.org/env/soe/.
- 11. NWDC Quarterly Economic Data Report (EDR), Quarter 2 of 2015/2016. NWDC Research and Innovation Unit, 2015. Available at: https://nwdc.co.za/economic-data-reports/.
- 12. NWDC Quarterly Economic Data Report (EDR), Quarter 2 of 2017/2018. NWDC Research and Innovation Unit, 2017. Available at: https://nwdc.co.za/economic-data-reports/.
- 13. NWDC Quarterly Economic Data Report (EDR), Quarter 2 of 2018/2019. NWDC Research and Innovation Unit, 2018 Available at: https://nwdc.co.za/economic-data-reports/.
- 14. NWDC Quarterly Economic Data Report (EDR), Quarter 2 of 2021/2022. NWDC Research and Innovation Unit, 2021. Available at: https://nwdc.co.za/economic-data-reports/.
- 15. NWDC Quarterly Economic Data Report (EDR), Quarter 3 of 2021/2022. NWDC Research and Innovation Unit, 2021. Available at: https://nwdc.co.za/economic-data-reports/.
- 16. Qi J., Chehbouni A., Huete A. R., Kerr Y. H., Sorooshian S. A modified soil adjusted vegetation index. *Remote Sensing of Environment*, 1994. Vol. 48, No. 2. P. 119–126. https://doi.org/10.1016/0034-4257(94)90134-1.
- 17. Qiu L., Chen Y., Wu Y., Xue Q., Shi Z., Lei X. et el. The Water Availability on the Chinese Loess Plateau since the Implementation of the Grain for Green Project as Indicated by the Evaporative Stress Index. *Remote Sensing*, 2021. Vol. 13, No.16, 3302. https://doi.org/10.3390/rs13163302.
- 18. Running S., Mu Q., Zhao M. MOD16A2 MODIS/Terra Net Evapotranspiration 8-Day L4 Global 500m SIN Grid V006 NASA EOSDIS Land Processes DAAC. 2017. https://doi.org/10.5067/MODIS/MOD16A2.006.
- 19. Shao H., Liu M., Shao Q., Sun X., Wu J., Xiang Z. et al. Research on eco-environmental vulnerability evaluation of the Anning River Basin in the upper reaches of the Yangtze River. *Environmental Earth Sciences*, 2014. Vol. 72 P.1555–1568. https://doi.org/10.1007/s12665-014-3060-9.
- 20. Statistics South Africa 2011. Census 2011 Provincial profile: North West. Report no. 03-01-75, Statistics South Africa, Pretoria. Available at: http://www.statssa.gov.za/publications/Report-03-01-75/Report-03-01-752011.pdf.
- 21. Sun H., Liu H., Ma Y., Xia Q. Optical remote sensing indexes of soil moisture: Evaluation and improvement based on aircraft experiment observations. *Remote Sensing*, 2021. Vol.13, No. 22, 4638. https://doi.org/10.3390/rs13224638.
- 22. Wang W., Sun. Y, Wu J. Environmental warning system based on the DPSIR model: A practical and concise method for environmental assessment. *Sustainability*, 2018. Vol. 10, No. 6, 1728. https://doi.org/10.3390/su10061728.
- 23. Longstaff B.J., Carruthers T.J.B., Dennison W.C., Lookingbill T.R., Hawkey J.M., Thomas J.E. et al. Integrating and applying science: A handbook for effective coastal ecosystem assessment. IAN Press, Cambridge, Maryland, 2010. P. 61-77. Available at: https://ian.umces.edu/publications/integrating-and-applying-science-a-handbook-for-effective-coastal-ecosystem-assessment/.
- 24. The spatial distribution of population in 2018, South Africa. WorldPop. Global High Resolution Population Denominators Project Funded by The Bill and Melinda Gates Foundation (OPP1134076). https://dx.doi.org/10.5258/SOTON/WP00645.
- 25. Zhang K., Thapa B., Ross M., Gann D. Remote sensing of seasonal changes and disturbances in mangrove forest: A case study from South Florida. *Ecosphere*, 2016. Vol. 7, No. 6, P. 1–23. https://doi.org/10.1002/ecs2.1366.
- 26. Zou T., Chang Y., Chen P., Liu J. Spatial-temporal variations of ecological vulnerability in Jilin Province (China), 2000 to 2018. *Ecological Indicators*, 2021 Vol. 133, 108429. https://doi.org/10.1016/j.ecolind.2021.108429.